Truth bomb :- Berry Curvature can be measured even at room temperatures.

Recap :- ① B. curv. affects electron dynamics

② $\sigma_H = \nu \frac{e^2}{\eta}$

ν: Chern # ⇒ is going to be integer

③ Symmetry properties

$\Omega(\vec{k}) = -\Omega(-\vec{k})$ TR

$\Omega(\vec{k}) = \Omega(-\vec{k})$

$\Omega(\vec{k}) = 0$

$C \neq 0$ only when TRS is broken

Todays agenda :- Valley hall effect in MoS_2 (cousin of graphene)

↓

detection of QHall effect

→ graphene like system, honeycomb lattice

=> "has Gap" 2 in #

⇒ turns out valleys, have opposite Berry curvature.

↙ electrons belonging to 1 valley get deflected to 1 side

↘ electrons on other side get deflected to other side.

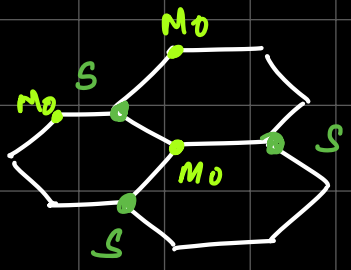

Instead of 1 layer, it has 3 layers

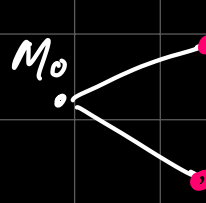

↑ on top of each other.

one molecule thick not 1 atom thick as in graphene

$\therefore \Omega(\vec{k}) \neq 0$ [We know that it'll happen, dirac eqn]

⇒ TB

⇒ effective hamiltonian.

S → essentially separate into ↑ + ↓

-S

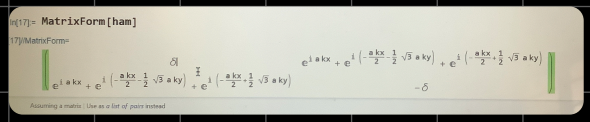

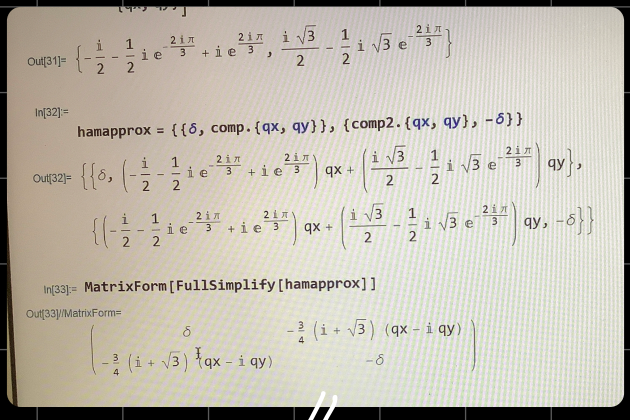

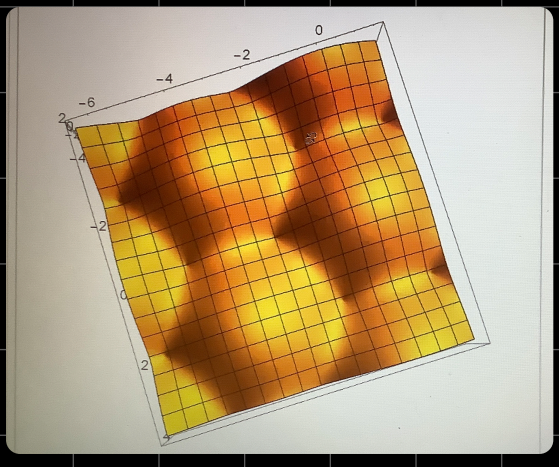

will be different for both valleys ⟶ dispersion is same

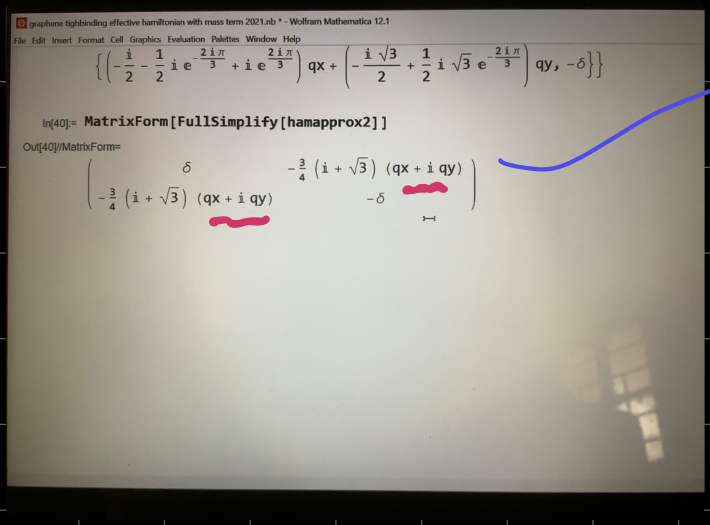

$\therefore$ CB bond in 1 valley has same eigenvector as VB in the other valley.

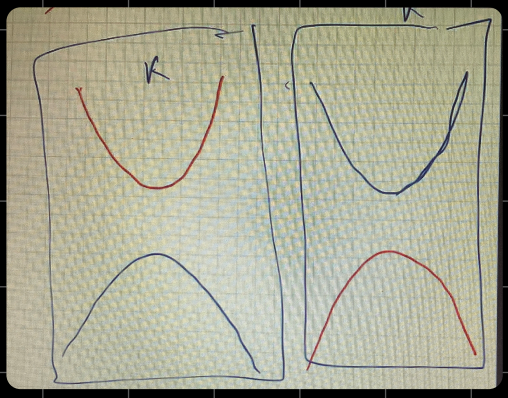

$\Omega \rightarrow$ on one valley

$-\Omega \rightarrow$ on another valley

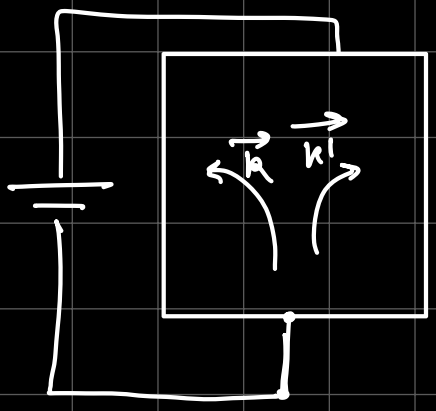

Valley filter

For graphene $\Rightarrow$ IR+TRS

$\Downarrow$

B. Curv. is 0.

$\Downarrow$

happens only because the Berry curvature is non-zero

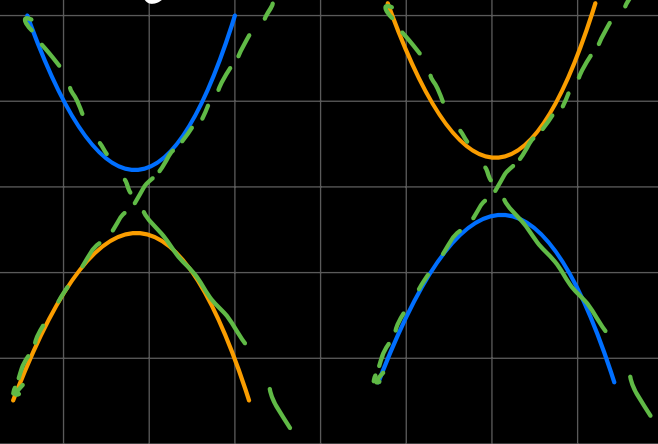

Check only that state possesses Berry curvature $\rightarrow$ however DOS is 0 here.

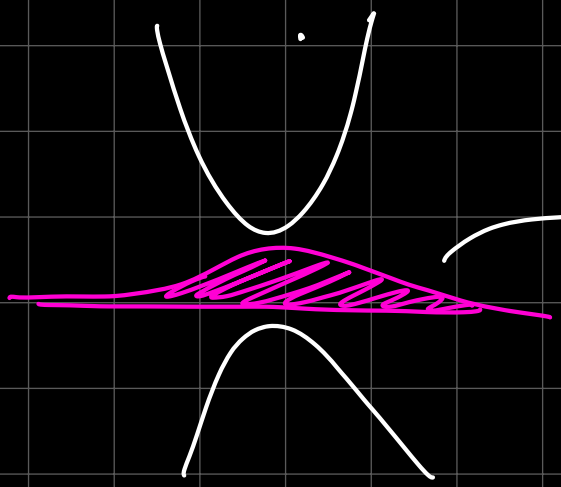

→ Berry curvature

File Edit Insert Format Cell Graphics Evaluation Palettes Window Help

$\sqrt{d^2 + x^2 + y^2}$

In[•]:=
```
berrycurvature = Im[bc[[3]] / ((2) * √(d^2 + x^2 + y^2))^2]
```
Out[•]= $-\frac{1}{2}\,\text{Re}\left[\frac{d}{(d^2 + x^2 + y^2)^{3/2}}\right]$

In[•]:=
```
Integrate[d * r / (2 (r^2 + d^2)^(3/2)), {r, 0, Infinity}, {t, 0, 2 π}]
```
Out[•]= $\frac{d\,\pi}{\text{Abs}[d]}$ if $d \neq 0$

In[•]:=
```
Integrate[d * r / (2 (r^2 + d^2)^(3/2)), {r, 0, rθ}, {t, 0, 2 π}]
```
Out[•]= $d\,\pi\left(-\frac{1}{\sqrt{d^2 + r\theta^2}} + \frac{1}{\text{Abs}[d]}\right)$ if $d \neq 0 \&\& \text{Re}[r\theta] \geq 0 \&\& \text{Im}[r\theta] == 0$

In[42]:=
```
Plot[1 / (d^2 + x^2 + y^2)^(3/2) /. d → 1 /. x → 0, {y, -5, 5}]
```
Out[42]=

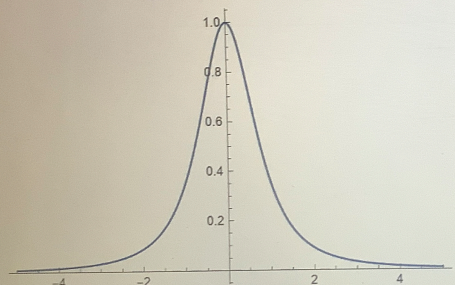

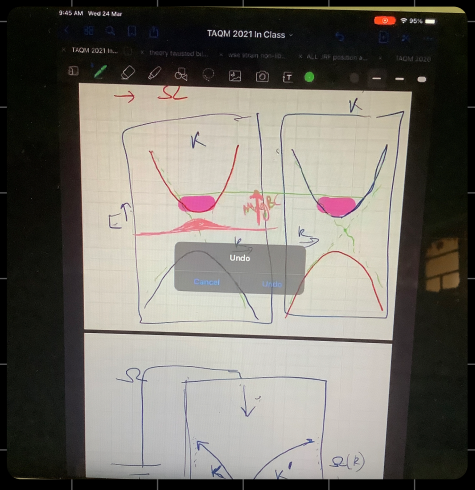

Cute trick →

Shine circularly polarized light couples to 1 valley → hence creates an imbalance

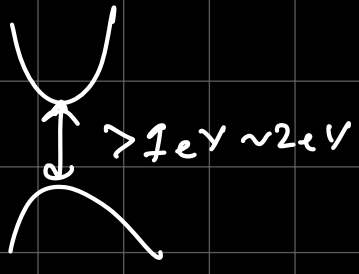

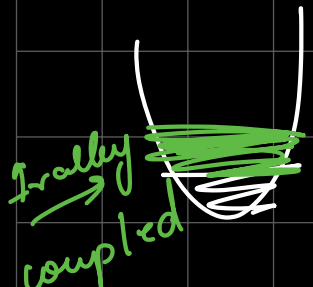

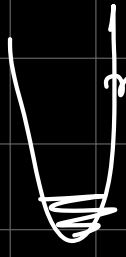

now due to unequal # of charge carriers in 2 valleys, we measure a voltage difference.

f valley-polarized carriers (*11*, *29*). Shown in the nset is the photocurrent ΔI_x as a function of V_x at V_g = 0 V) under different laser excitation in-

from right- to left- handed, or θ =–45°, in which the polarization is modulated from left- to right-handed, we use the notations R-L and L-R below,

of a net valley polarization under the optical excitation of the A resonance with circularly polarized light (*10*–*14*). The sine dependence of

ig. 1. Monolayer MoS_2 Hall ar device. (**A**) Schematics of e valley-dependent optical election rules and the electrons the K and K′ valleys that ossess opposite Berry urvatures Ω. The orange rrows represent the clockwise nd counterclockwise hopping otions of the K and K′ ectrons. (**B**) Schematic of a notoinduced AHE driven by a et valley polarization (left) and n image of the Hall bar device ight). In the schematic, the trinsic plus side-jump ontribution as predicted by q. 1 is shown. (**C**) Two-point ashed line, V_x = 0.5 V) nd four-point (solid line) onductivities of the device as a nction of back gate voltage V_g. nset) Source-drain bias (V_x) ependence of the current along e longitudinal channel (I_x) at

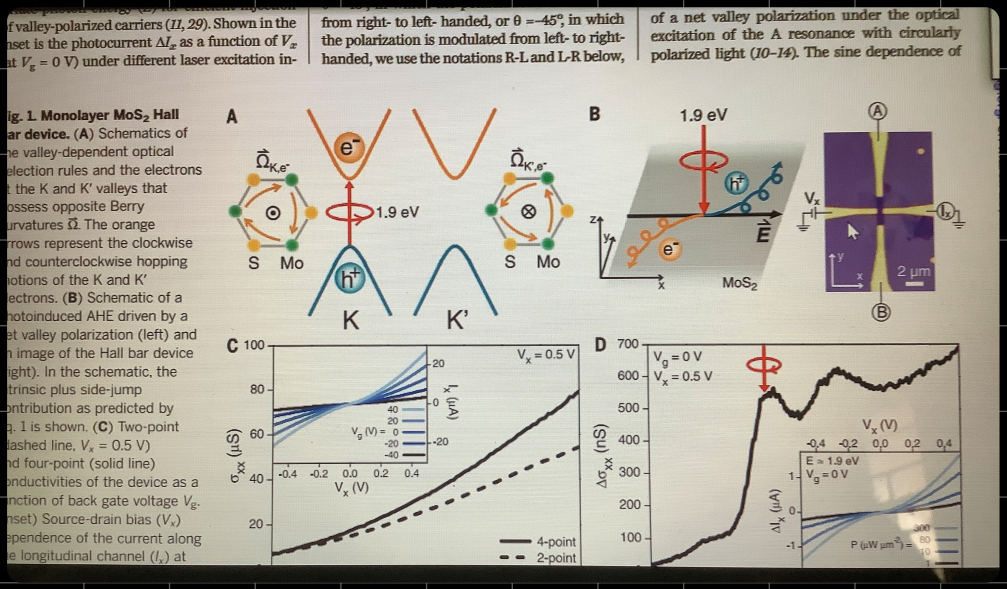

der on-resonance excitation and is shown in Fig. 2A [electrical characterization of our bilayer device is provided in (*23*), section 2.7]. No noticeable Hall voltage (more than a factor of 10

intervalley population

drive the AHE. No such imbalance can be produced in bilayer MoS_2 (*4*–*6*) because the inversion symmetry is restored in its crystal structure (*11*, *14*, *31*).

Last, the effect of the intervalley relaxation of excited carriers on the AHE in MoS_2 monolayers is depicted in Fig. 2C. The dependences of the anomalous Hall conductivity $\sigma_H = \frac{\Delta\sigma_{xx}}{\Delta\sigma_{xx}^2 + \sigma_{xx}^2} R_H \sigma_{xx}^2$ and of the change in conductivity $\Delta\sigma_{xx}$ on the incident photon energy E are shown, whereas $\Delta\sigma_{xx}$ remains linear and keeps increasing with increased photon energy beyond the A and B resonances (thanks to an enhancement in optical absorption), the anomalous Hall conductivity σ_H peaks near the A feature and decreases quickly to almost zero at higher photon energies. Our observation is consistent with recent optical results that indicate poor injection of valley polarization under off-resonance excitation because of the rapid intervalley relaxation of high-energy excited carriers (*11*, *29*). For comparison, no detectable Hall conductivity is observed in the bilayer device (Fig. 2C, blue dots).

Our experimental observation of a finite AHE only in monolayer MoS_2 under on-resonance, circularly polarized excitation strongly supports our interpretation of the signal as originating from the VHE. Whereas a net spin polarization could also give rise to a finite AHE, the effect

intensity (P) dependence of the p
AHE under 1.9 eV excitation. For th
measured the gate dependence o
different incident laser powers [(2
2.9]. The effective change in the ph
carrier density Δn_{ph} can then be estim
the relation $\Delta\sigma_{xx} = \Delta n_{ph} e\mu$, where μ
extracted from the dark electrical me
(Fig. 1C) with $C_g = 1.2 \times 10^{-8}$ F cm^{-2}
gate capacitance of our device (Δn_{ph}
ficult to measure with conventiona
methods because of a large backgro
density and finite longitudinal-tra
pling in our devices). The quantity
be equal to Δn_v if the change in cond
is solely driven by the valley-polar
that are directly excited by resona
polarized light. In reality, howeve
include contributions from both va
and -unpolarized carriers; therefo
vides an upper bound for Δn_v. Th
Hall conductivities under R-L m
different gate voltages V_g are show
of Δn_{ph} in Fig. 3. We also show t
result predicted by Eq. 1 in the lin
in the same figure. For all gate v
creases linearly with Δn_{ph}, whic
with the theoretical prediction. T
Hall conductivity σ_H also has the

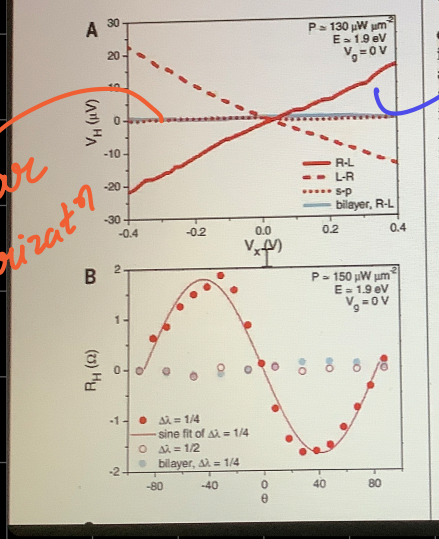

linear polarizat^n

Circular polarization

bilayer MoS_2 → doesn't break Inv. symmetry

Trilayer MoS_2 ↪ breaks Inv. symmetry

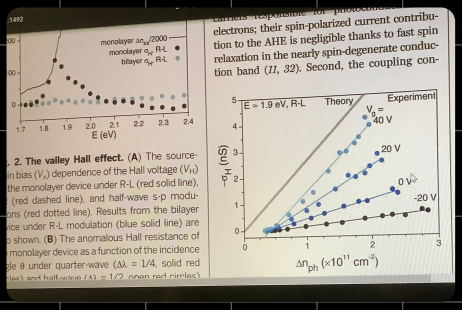

2. The valley Hall effect. (**A**) The source-in bias (V_x) dependence of the Hall voltage (V_H) the monolayer device under R-L (red solid line), (red dashed line), and half-wave s-p modu-ons (red dotted line). Results from the bilayer ice under R-L modulation (blue solid line) are shown. (**B**) The anomalous Hall resistance of monolayer device as a function of the incidence gle θ under quarter-wave (Δλ = 1/4, solid red

electrons; their spin-polarized current contribu-tion to the AHE is negligible thanks to fast spin relaxation in the nearly spin-degenerate conduc-tion band (*11*, *32*). Second, the coupling con-

So Berry phase/curvature have been tested in expt settings.

Buzzwords ⇒ berry curvature dipole

Strain → uniaxial strain → if berry curvature hotspots don't cancel each other.

Comment
↳ hotspots of BC are just at the degeneracy points & hence don't affect stuff at large k pnts.

MoS_2 Dan Ralph problem

$$H_K = \delta\sigma_z + v_f(\sigma_x k_x + \sigma_y k_y) \longrightarrow IR^{\checkmark}, TRSX$$

$$H_{K'} = \delta\sigma_z + v_f(-\sigma_x k_x + \sigma_y k_y) \longrightarrow IR^{\checkmark}, TRSX$$

K

$$H = \begin{pmatrix} \delta & v_f(k_x - ik_y) \\ v_f(k_x + ik_y) & -\delta \end{pmatrix}$$

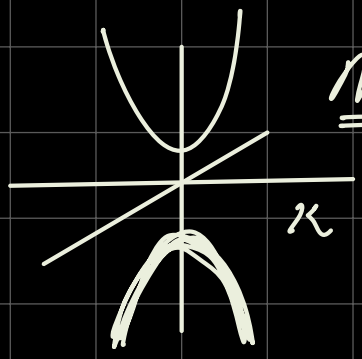

MoS_2

$$\mathcal{E} = \pm\sqrt{v_f^2(\vec{k}\cdot\vec{k})_{2D} + \delta^2}$$

BC:- $p = |E_f|$ $\quad H = p\begin{bmatrix} \cos\theta & \sin\theta e^{-i\phi} \\ \sin\theta e^{i\phi} & -\cos\theta \end{bmatrix}$

ev =

$$|\uparrow\rangle = \begin{pmatrix} e^{-i\phi}\cos\theta/2 \\ \sin\theta/2 \end{pmatrix}\frac{x\hat{1}}{\sqrt{2}} \qquad |\downarrow\rangle = \mathcal{T}|\uparrow\rangle = \begin{pmatrix} +\sin\theta/2 \\ -e^{i\phi}\cos\theta/2 \end{pmatrix}$$

where $\cos\theta = \frac{S}{E_+}$ $\sqrt{\frac{v_f^2(k_x^2+k_y^2)}{E_+^2}} = |\sin\theta|$

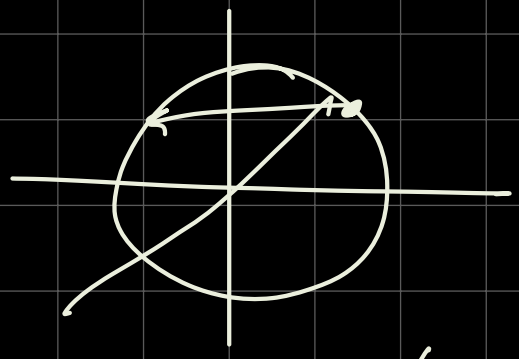

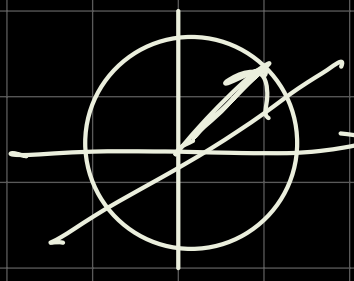

$p \sin\theta \cos\phi$

$p \sin\theta \sin\phi$

$\phi \to \phi + \pi$

$$|\uparrow\rangle = \begin{pmatrix} e^{-i\phi}\cos\theta/2 \\ \sin\theta/2 \end{pmatrix} \times \frac{1}{\sqrt{2}}$$

$A_\phi = \left(\frac{1}{2}\right)\cos^2\theta/2$ $\qquad A_\theta = 0$

$$F_{\theta\phi} = \frac{\partial A_\theta}{\partial \phi} - \frac{\partial A_\phi}{\partial \theta} = +\cos\theta/2\left(\frac{1}{2}\right)\sin\theta/2 = \frac{1}{4}\sin\theta$$